

Original Article

Feasibility of carotid artery PET/MRI in psoriasis patients

Prabhakar Rajiah^{1,2}, Mojgan Hojjati¹, Ziang Lu¹, Vijaya Kosaraju¹, Sasan Partovi¹, James K O'Donnell¹, Christopher Longenecker³, Grace A McComsey⁴, Jackelyn B Golden⁵, Fuad Muakkassa⁵, Scott Santilli⁵, Thomas S McCormick⁵, Kevin D Cooper⁵, Neil J Korman⁵

¹Department of Radiology, University Hospital Cleveland Case Medical Center, Case Western Reserve University School of Medicine, Cleveland, Ohio, United States; ²Department of Radiology, Cardiothoracic Imaging, UT Southwestern Medical Center, Dallas, Texas, United States; ³Department of Cardiology, University Hospital Cleveland Case Medical Center, Case Western Reserve University School of Medicine, Cleveland, Ohio, United States; ⁴Department of Pediatrics and Medicine, University Hospital Cleveland Case Medical Center, Case Western Reserve University School of Medicine, Cleveland, Ohio, United States; ⁵Department of Dermatology, University Hospital Cleveland Case Medical Center, Case Western Reserve University School of Medicine, Cleveland, Ohio, United States

Received April 8, 2016; Accepted June 29, 2016; Epub August 20, 2016; Published August 30, 2016

Abstract: We report our initial experience of performing integrated PET/MR imaging of the carotid arteries in psoriatic patients. Eleven patients with psoriasis and ten controls underwent carotid PET/MRI. Following injection of the FDG tracer, 3d T1w gradient echo sequence (atMR) was obtained for attenuation correction of PET data. High resolution images of carotid artery were then obtained, including pre-and post-contrast T1-w, T2-w and proton-density images as well as TOF images followed by PET imaging of the torso. From the fused axial PET/MRI, the arterial wall SUVmax and TBRmax was quantified in each slice. MRI images were also evaluated for vessel wall volume, plaque and internal composition. SUVmax and TBRmax were respectively, 1.72 ± 0.38 & 1.17 ± 0.27 in L-CCA, 1.75 ± 0.39 & 1.24 ± 0.19 in R-CCA, 1.59 ± 0.24 & 1.08 ± 0.14 in L-ICA and 1.62 ± 0.27 & 1.15 ± 0.17 in R-ICA in psoriatic patients and 1.74 ± 0.22 & 1.28 ± 0.44 in L-CCA, 1.74 ± 0.33 & 1.07 ± 0.28 in R-CCA, 1.78 ± 0.32 & 1.29 ± 0.39 in L-ICA and 1.60 ± 0.29 & 0.98 ± 0.25 in R-ICA in the controls. No discrete plaques were identified in any of the vessel segments in MRI. PET/MRI is feasible in evaluation of carotid arteries in psoriatic patients.

Keywords: Psoriasis, PET, MRI, atherosclerosis, inflammation, carotid

Introduction

Psoriasis is a chronic, inflammatory, immune-mediated disease of unknown etiology, prevalent among 3.2% of adults in the United States [1-3]. Patients with plaque psoriasis demonstrate characteristic skin erythema driven by endothelial cell growth, and epidermal hyperproliferation resulting in a build-up of shed keratinocytes (often referred to as "scale"). In addition to keratinocyte alterations, an increase in epidermal CD8+ T lymphocytes and dermal CD4+ cells, dendritic cells (DCs), monocytes, macrophages, and neutrophils is observed [4]. Increased levels of T cells and monocytes, along with corresponding inflammatory cytokines such as IL-6, IL-12, IL-23, and IL-17A, are

also present in circulation [5-8]. Psoriasis patients exhibit numerous co-morbid conditions including psoriatic arthritis, obesity, diabetes, and an increased propensity to develop cardiovascular disease such as atherosclerosis, myocardial infarction, and stroke [9-14].

Atherosclerosis, especially in young patients, usually remains asymptomatic and presents with subclinical increase of arterial intima and media thickness until it has reached an advanced phase [15]. However, even asymptomatic patients with significant stenosis can be at risk for stroke. As a result, non-invasive identification of both early precursor and advanced deposition of atherosclerotic plaques is of clinical value [16].

Carotid PET/MRI in psoriasis patients

¹⁸F-fluorodeoxyglucose (FDG) positron emission tomography (PET) has emerged as a potential imaging modality for the detection of increased metabolic activity associated with macrophage recruitment and activation, neo-angiogenesis, and resultant inflammation and vessel plaque formation [17-19]. Due to the association between psoriasis and increased risk of atherosclerosis, early endothelial atherosclerotic changes in psoriatic patients may be visualized as an increase in endothelial ¹⁸F FDG uptake on PET [16]. In addition to ¹⁸F-FDG PET, magnetic resonance imaging (MRI) may also play a role in the detection of inflammatory cardiovascular plaques, as it has been effective in the visualization and determination of plaque components [4, 11, 12, 20, 21].

Despite the utility of these two imaging modalities, combined ¹⁸F-FDG PET and MR imaging presents several logistical difficulties, including maintaining patient placement and neck angulation for co-localization of anatomy [16]. However, several hybrid PET/MRI systems have been introduced to clinical practice, targeting these technical challenges concerning the co-registration of PET and MRI data. As a result, PET/MR may be used as a viable alternative to PET/CT for non-invasive imaging of atherosclerosis, as MRI has superior soft tissue characterization and targets vessel wall, potential atherosclerotic plaques, and sub components within the vessel wall, while CT primarily visualizes the lumen [19]. PET/MR also limits patient radiation exposure compared to PET/CT. However, PET/MR is restricted in terms of attenuation correction, as MR attenuation maps are not directly collected from target tissue. Rather, they are estimated based on acquired tissue densities without consideration for bone-potentially influencing the quantification of PET images. This may be problematic as carotid arteries are in proximity to the cervical spine [1, 22-26].

The aim of this study was to evaluate the feasibility of integrated PET/MR imaging of the carotid arteries in psoriatic patients.

Materials and methods

Ethical approval

This HIPAA-compliant study was approved by our institutional review board (IRB). All subjects received verbal and written information regard-

ing the study and expressed written informed consent before inclusion.

Study design, patient population

Eleven patients with moderate to severe psoriasis (9 male and 2 female, median age 40.0 years (range: 21.0-65.0), 9 Caucasians and 2 African Americans) were prospectively recruited from our dermatology outpatient clinic. The median psoriasis area and severity index (PASI) for these eleven patients was 22.8 (range: 18.0-42.6) with a median duration of disease of 14.0 years (range: 1.0-48.0). Ten-year Framingham risk scores were calculated using the NIH online calculator (<http://cvdrisk.nhlbi.nih.gov/>) taking into account age, gender, total cholesterol, HDL cholesterol, smoking history, systolic blood pressure, and patient history of blood pressure medication.

Inclusion criteria were 1) diagnosis of moderate-to-severe psoriasis that affected $\geq 10\%$ of the subject's body surface area (BSA), 2) age 18-65 years and 3) willingness to complete a washout period to discontinue systemic therapies for at least 4 weeks and topical and phototherapies for at least 2 weeks prior to beginning of study.

Exclusion criteria were 1) subjects currently on a therapeutic regimen and unwilling to go through the washout period, 2) subjects with a critical illness or who were immunocompromised, 3) age <18 years or weight >400 pounds, 4) currently pregnant or breastfeeding, 5) subjects who have metal implants, a pacemaker, stent, or artificial heart valve, 6) have a history of clinically significant hematological, renal, or liver disease, or 7) history of myocardial infarction (MI), cerebrovascular accident (CVA), or significant atherosclerosis (defined as the presence of any carotid plaque, or carotid intimal media thickness (cIMT) >75th percentile for age, or the presence of coronary artery calcium score >100).

Ten controls without any cardiovascular disease were also scanned (9 males, 1 female, median age- 45.3 years (range: 21-61), 6 Caucasians and 4 African Americans).

Patient preparation

After fasting for at least 6 hours, all the patients underwent carotid PET/MR following injection of 4.44×10^8 Bq ¹⁸F-FDG through a cubital vein

Carotid PET/MRI in psoriasis patients

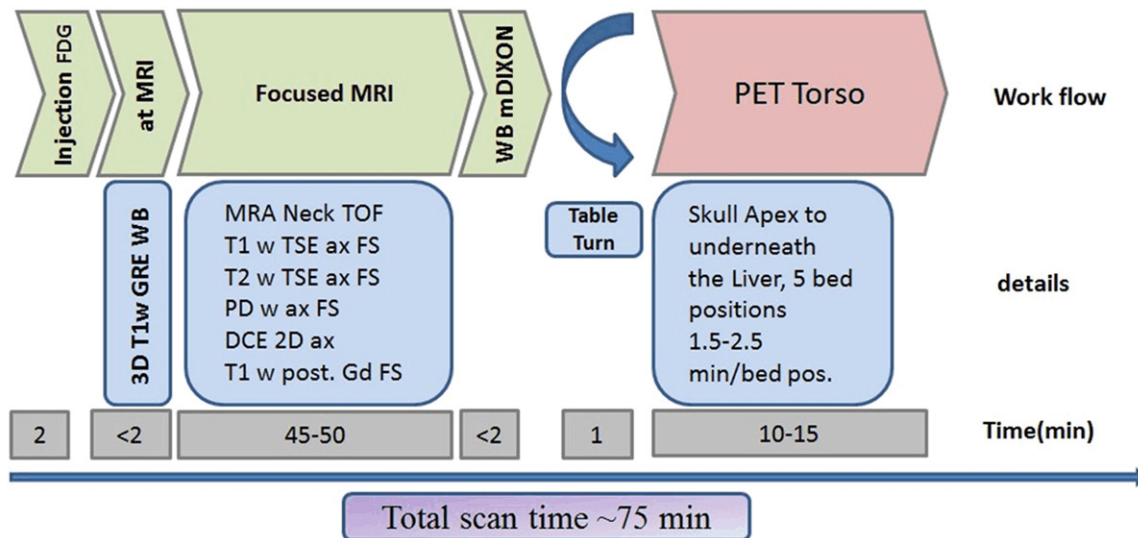


Figure 1. Workflow of carotid artery PET/MRI in psoriasis patients. After injection of FDG, 3d T1 weighted attenuation corrected MRI images are obtained. This was followed by dedicated MRI sequences, which consisted of 3d-Time of flight, T1-w, T2-w, PD-weighted black blood images before contrast. After contrast administration, dynamic enhanced images and T1-weighted axial images were obtained. Following this, FDG PET torso acquisition was performed.

catheter. Plasma glucose measured before injection ranged from 4.0 to 6.0 mmol/l. Patients avoided speaking and rested in a temperate and quiet environment from 15 minutes pre-injection to 30 minutes post-injection to reduce tracer uptake in both neck and mouth musculature and brown fat regions.

PET/MR acquisition

The PET/MR examination was performed on a sequential PET/MR scanner system (Ingenuity TF PET/MRI, Philips Healthcare) using a dedicated head and neck coil (Philips Healthcare) [27, 28]. The PET/MRI workflow is illustrated in **Figure 1**. Following intravenous injection of ^{18}F -FDG, patients were placed in the scanner and underwent imaging. Scout images were acquired to localize the carotid arteries before a 3d T1-weighted multi-station spoiled gradient echo sequence (atMR) of the torso was obtained for attenuation correction of PET data (MRAC), deriving from a 3-segment model accounting for soft tissue, lung tissue, air, and fat. Following this, targeted high resolution imaging of the carotid arteries was performed. A 3D time-of-flight (TOF) bright magnetic resonance angiography sequence (TR/TE 23/3.5 ms, flip angle 20°) was initially performed to visualize the carotid lumen contours. 12 axial high-resolution images of the carotid arteries were obtained, centered on the carotid bifurca-

tion based on the 3d-TOF angiography, with 6 slices cranial and 6 slices caudal to the carotid bifurcation. Proton-density, T1-w and T2-w images were then obtained using fat-suppressed black-blood double inversion recovery sequences with slice thickness of 3 mm and matrix size of 256 x 234. The sequence parameters for T1-w images were: TR/TE -1091/10 ms; echo train length - 13; T2-w images: TR/TE -2182/80 ms; echo train length-20; proton density-w images: TR/TE- 3073/20 ms; echo train length- 8. After administration of gadolinium-based intravenous contrast media (0.1 mmol/kg), dynamic contrast enhanced images were obtained followed by T1-weighted double inversion recovery sequence. After MRI is completed, FDG-PET imaging of the torso was performed. The median time between FDG tracer injection and PET acquisition was approximately 55-60 minutes. FDG-PET imaging (10-15 minutes for five bed positions) was acquired through the neck and torso, after which mDixon images of the torso (slice thickness 3 mm) were obtained for anatomical correlation with PET imaging. The total average examination time of the PET/MRI was 75 minutes.

Image reconstruction and data analysis

Based on attenuation maps and automatic rigid registration, PET/MR images were recon-

Carotid PET/MRI in psoriasis patients

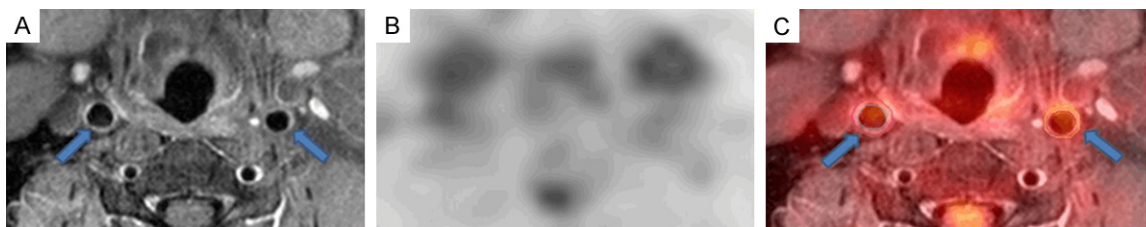


Figure 2. Transverse T1 weighted MRI image (A), PET image (B) and fused FDG-PET/MR (C) at the level of the right and left common carotid artery (blue arrows). Arterial-wall FDG uptake was quantified by drawing two region of interests (ROI) around the lumen and outer wall of each CCA (right and left) on fused FDG-PET/MR images (B) to define the wall area. Maximum standard uptake value of the carotid wall was then calculated using MIM software, which was corrected for blood pool activity (jugular vein) to obtain TBR.

Table 1. Baseline characteristics of psoriasis patients

Characteristics	n=11 median (range)
Male/Female	9/2
Age	40.0 (21.0-65.0)
Body mass index (BMI)	26.0 (20.9-44.4)
PASI score	22.8 (18.0-42.6)
Body surface area (BSA)	34.0 (15.0-83.5)
Duration of disease (years)	14.0 (1.0-48.0)
Framingham risk score (%)	3.0 (1.0-15.0)
Family history of ischemic heart disease	2
History of smoking	5
Known Hypertension	2
Diabetes	1
Known Cardiovascular Disease	0
Deep Venous Thrombosis	1
hsCRP	6.2 (0.8-17.6)

structured and analyzed by a board certified radiologist. MR-based PET attenuation correction maps (MR-AC) (**Figure 2A**) was fused with the T1-weighted TSE black blood images (**Figure 2B**). Arterial-wall FDG uptake was quantified on axial fused PET/MR images using commercially available software (MIM Software™, version 6.1 Cleveland, Ohio) by drawing regions of interest (ROIs) in the common and internal carotid arteries, including the vessel wall and excluding the lumen (**Figure 2C**). Maximal, mean, median, and standard deviation of standard uptake value (SUV) were measured along the common and internal carotid arteries for each axial slice. SUV is calculated as a time-corrected concentration of tissue radioactivity in kilobecquerels (kBq) per mL, adjusted for injected FDG dosage and body weight of the patient, and is a widely used method for quantification of FDG-PET data [29].

For evaluation of the FDG blood pool uptake, ROIs were drawn in jugular veins. The maximal arterial target to background Ratios (TBRs) were then calculated by dividing the maximal arterial SUVs by the blood pool SUV, estimated from jugular vein ROIs, to produce a background-corrected carotid arterial SUV. The MRI images were also evaluated for vessel wall volume, presence of plaque, and if plaque was present - for internal composition, including fat and edema.

Statistical analysis

Statistical analysis was performed using R (Version 3.2.2). GraphPad Prism 6 software was used for graph generation. Categorical data was described as means and standard deviations. SUVmax and TBRmax differences were analyzed by Welch 2-sample t-test with 95% confidence interval. Statistical differences were set to $p < 0.05$. The correlations between SUVmax and TBRmax values of ICA segments on the same side were analyzed by Spearman correlation coefficient

Results

The characteristics of psoriasis patient cohort at baseline, including disease severity and duration are shown in **Table 1** with a 10-year Framingham risk value and additional risk factors associated with prevalence of cardiovascular disease described.

For the psoriatic patients, total of 252 carotid vessel segments were analyzed. A total of 35 left common carotid artery (LCCA), 91 left internal carotid artery (LICA), 31 right common carotid artery (RCCA), and 95 right internal

Carotid PET/MRI in psoriasis patients

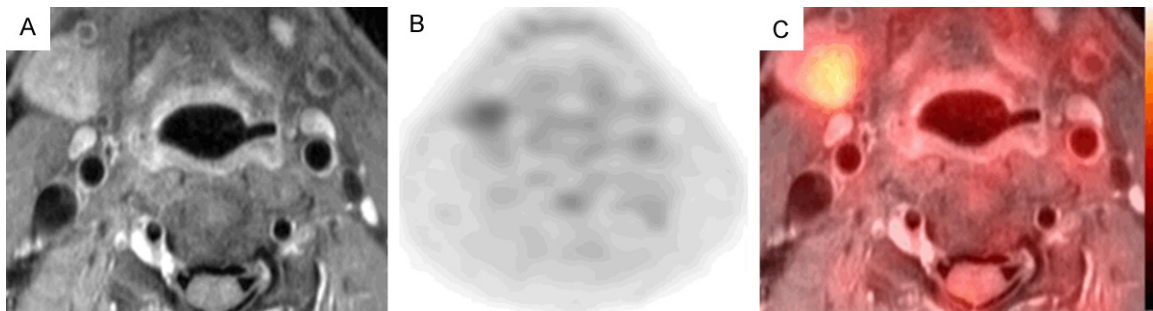


Figure 3. Example of carotid PET/MRI from another patient. A. Axial T1-w MRI image at the level of common carotid artery. B. MRAC PET non-fused image of the neck. C. PET/MRI images with fused MRAC PET and T1 w black blood images demonstrate FDG activity.

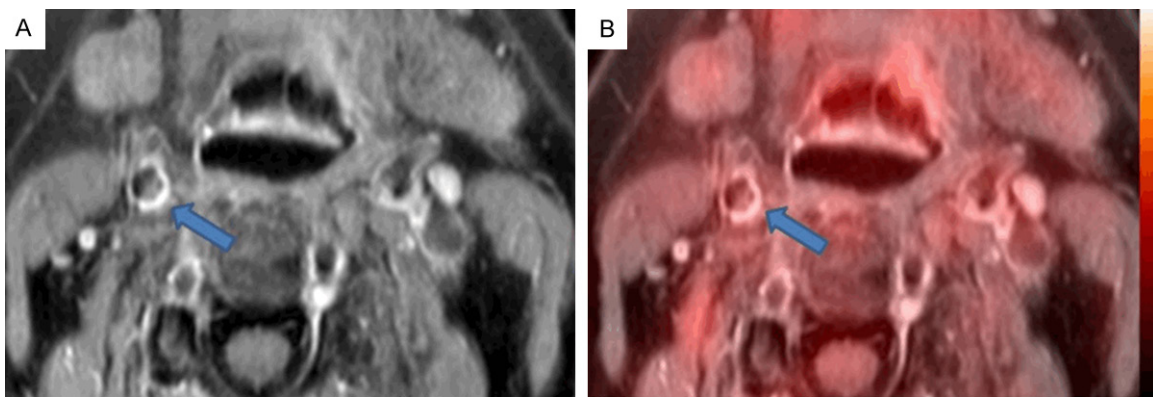


Figure 4. A. Axial T1-weighted turbo spin echo (black blood) image shows high signal in the right common carotid artery (Blue arrow). B. Fused PET/MRI image in the same patient at the same level showed mild increased SUVmax at this level.

Table 2. Summary of the mean, minimum, maximum and standard deviation of whole vessel SUV and TBR maximum values within each vessel segment analyzed

VESSEL SEGMENT		PSORIASIS (N=11) (Mean ± SD (Min, Max))	CONTROLS (N=10) (Mean ± SD (Min, Max))	p-Value
LICA	SUVmax	1.59 ± 0.24 (1.1, 1.9)	1.78 ± 0.32 (1.4, 2.4)	0.15
	TBRmax	1.08 ± 0.14 (0.9, 1.3)	1.29 ± 0.39 (0.52, 2.0)	0.13
LCCA	SUVmax	1.72 ± 0.38 (1.2, 2.4)	1.74 ± 0.22 (1.4, 2.1)	0.86
	TBRmax	1.17 ± 0.27 (0.8, 1.7)	1.28 ± 0.44 (0.56, 2.1)	0.51
RICA	SUVmax	1.62 ± 0.27 (1.2, 2)	1.60 ± 0.29 (1.3, 2.1)	0.88
	TBRmax	1.15 ± 0.17 (0.9, 1.5)	0.98 ± 0.25 (0.36, 1.3)	0.08
RCCA	SUVmax	1.75 ± 0.39 (1.2, 2.4)	1.74 ± 0.33 (1.3, 2.3)	0.93
	TBRmax	1.24 ± 0.19 (0.9, 1.6)	1.07 ± 0.28 (0.36, 1.3)	0.12

LICA- Left internal carotid artery; LCCA- Left common carotid artery; RICA- Right internal carotid artery; RCCA- Right common carotid artery.

carotid artery (RICA) segments vessel slices were analyzed. For the control patients, total of 235 carotid vessel segments were analyzed. A total of 44 left common carotid artery (LCCA), 73 left internal carotid artery (LICA), 42 right common carotid artery (RCCA), and 76 right

internal carotid artery (RICA) segments vessel slices were analyzed. To accord equal weight to patients, standardized uptake value maximum values (SUVmax) and target to background ratio maximum values (TBRmax) were averaged to derive whole vessel SUVmax and

Left Sided Vessels

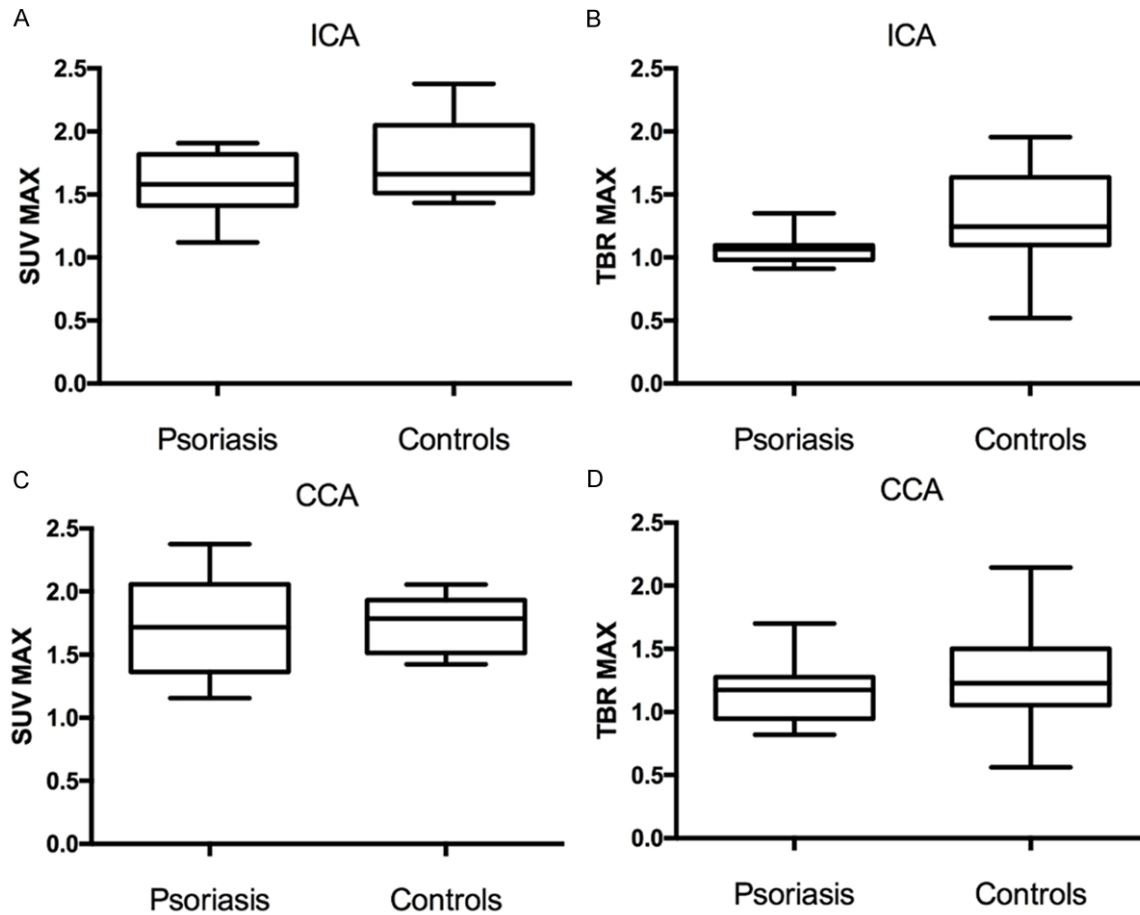


Figure 5. Box plots of absolute SUVMAX and TBRMAX values for left sided vessels comparing psoriasis patients with control group for ICA SUVMAX (A), ICA TBRMAX (B), CCA SUVMAX (C), and CCA TBRMAX (D). Box-plot edges indicate the 25th and 75th percentiles, central bars indicate medians and whiskers indicate extremes.

TBRmax values for each patient (**Figures 3, 4**). Values for whole vessel SUVmax and TBRmax are shown in **Table 2**.

The absolute SUVmax in psoriatic patients for LICA, LCCA, RICA and RCCA were 1.59 ± 0.24 , 1.72 ± 0.38 , 1.62 ± 0.27 , and 1.75 ± 0.39 respectively, which was not statistically different from SUVmax in controls, which were 1.78 ± 0.32 , 1.74 ± 0.22 , 1.60 ± 0.29 and 1.74 ± 0.33 respectively. Similar trends were also seen in TBRmax values. The absolute TBRmax in psoriatic patients for LICA, LCCA, RICA and RCCA were 1.08 ± 0.14 , 1.17 ± 0.27 , 1.15 ± 0.17 and 1.24 ± 0.19 respectively, which was not statistically different from TBRmax in controls, which were 1.29 ± 0.39 , 1.28 ± 0.44 , 0.98 ± 0.25 and 1.07 ± 0.28 respectively. P values are listed in **Table 2**. Boxplots compar-

ing SUVmax and TBRmax between psoriasis group and control group were shown in **Figure 5** for left sided vessels and **Figure 6** for right sided vessels. SUVmax and TBRmax values were higher in psoriasis group for RICA and RCCA without reaching statistical significance.

On correlating SUVmax and TBRmax for same vessels, significant correlations between LICA SUVmax and LCCA SUVmax ($r = 0.81$, $p = 0.004$), between LICA TBRmax and LCCA TBRmax ($r = 0.72$, $p = 0.016$), between RICA SUVmax and RCCA SUVmax ($r = 0.89$, $p = 0.0005$), and between RICA TBRmax and RCCA TBRmax ($r = 0.83$, $p = 0.0027$) were seen (**Figure 7**). On evaluation of the MRI images, there was no visible plaque in any of the evaluated vessel segments. There was no abnormal wall thickening or contrast enhancement.

Right Sided Vessels

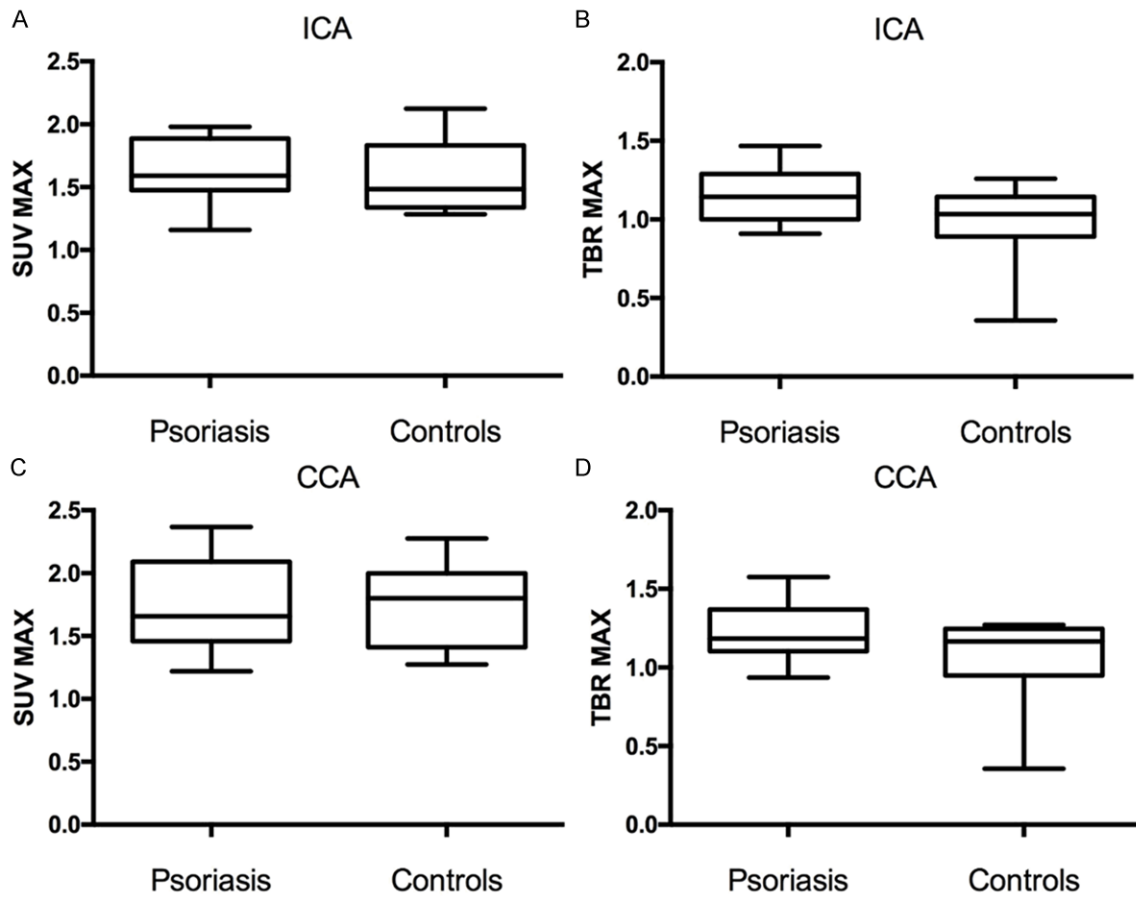


Figure 6. Box plots of absolute SUVMAX and TBRMAX values for right sided vessels comparing psoriasis patients with control group for ICA SUVMAX (A), ICA TBRMAX (B), CCA SUVMAX (C), and CCA TBRMAX (D). Box-plot edges indicate the 25th and 75th percentiles, central bars indicate medians and whiskers indicate extremes.

Discussion

To our knowledge this study is the first to investigate the use of carotid PET/MRI in the psoriatic patient population. Our study has demonstrated the feasibility of carotid PET/MRI for the assessment of metabolic changes in psoriatic patients.

Psoriasis is associated with increased atherosclerotic risk in different vascular beds, including carotid arteries and these patients have been shown to frequently present with carotid plaques [30, 31]. MRI enables carotid arterial wall delineation with high spatial and temporal resolution, which helps in accurate measurement of ^{18}F -FDG PET uptake, which is associated with atherosclerotic plaque inflammation [16, 17]. The superior visualization of the arte-

rial wall with MRI compared to CT, along with comparable lesion identification (3, 4) indicates the use of PET/MRI as an alternative for PET/CT in assessing early vascular metabolic changes associated with carotid atherosclerosis [19, 24]. This potentially allows safer and more effective early detection of plaque formation and assessment of subsequent cardiovascular risk in psoriasis patients.

The utility of FDG-PET/CT in assessment of vascular plaques in psoriatic patients has been studied, with increased SUVmax on PET/CT corresponding to plaque formation [32, 33]. PET/CT has also been used in establishing the relationship between ^{18}F -FDG uptake and reduction in vascular smooth muscle cells ultimately leading to collagen degradation and adventitia

Carotid PET/MRI in psoriasis patients

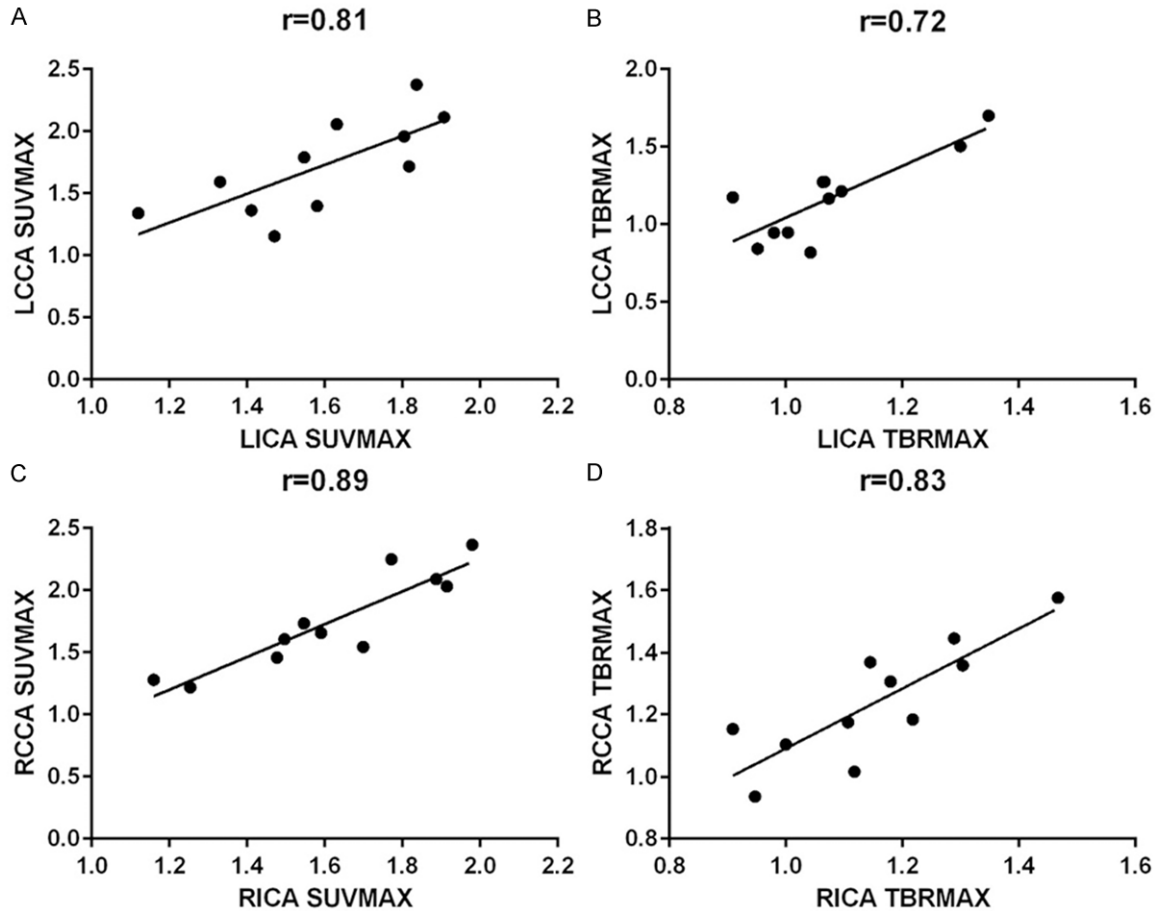


Figure 7. Correlation of SUVMAX and TBRMAX values between CCA and ICA vessels on the same side. A. Left CCA vs Left ICA SUVMAX; B. Left CCA vs Left ICA TBRMAX; C. Right CCA vs Right ICA SUVMAX; and D. Right CCA vs Right ICA TBRMAX. Significant positive correlations were demonstrated in all four segments (Spearman rank correlation test).

remodeling in atherosclerosis [29]. Furthermore, PET/CT has shown reduction in ^{18}F -FDG uptake of carotid arteries in psoriasis patients receiving tumor necrosis factor- α antagonist therapy (adalimumab) [34]. However, despite the established use of PET/CT for vascular plaque detection, PET/MRI may be more accurate for plaque detection and localization as well as assessment of novel therapeutics due to its focus on arterial wall rather than vascular lumen as measured in PET/CT [16]. Dave et al showed localization of inflammation detected in blood vessels by PET/CT in a psoriatic patient to the wall of the aorta when examined by PET/MRI [35].

A previous study has shown that FDG-PET/MRI is a feasible modality for assessment of increased carotid artery metabolic activity and, in turn, inflammation for subjects at risk for heart disease [36]. Increased TBR on PET/MRI

has been correlated to symptomatic atherosclerotic carotid plaques [37]. Furthermore, one study has shown strong association between significant findings on individual ^{18}F -FDG-PET and T1 weighted MRI and the presence of lipid-rich or hemorrhagic carotid plaques [38]. Such plaques may have an increased risk to rupture leading to cerebrovascular events, such a stroke. These studies indicate the potential diagnostic significance of PET/MRI for prediction of early development of carotid atherosclerotic plaques and detection of symptomatic carotid plaques in psoriasis patients.

Due to the capability of PET/MRI to predict early carotid plaque onset in patients with cardiovascular risk, this modality can emerge as an attractive hybrid imaging tool in psoriasis patients who face increased risk of atherosclerosis.

Our study has several limitations including the sample size, which is small. We present preliminary data only and further studies in larger patient populations is required. In addition, the patients in our study were relatively healthy psoriasis patients without a high risk for factors known to increase the risk of cardiovascular disease. This is the probable cause for no significant difference between psoriasis patients and controls in our study. This has also restricted the predictive ability of our study as we were only able to correlate ^{18}F -FDG uptake between internal and common carotids and ipsilateral carotid artery segments without further comparison of SUVmax and TBRmax between carotid plaques. Since we did not have PET/CT data, we could not correlate ^{18}F -FDG uptake in PET/MRI and PET/CT and quantify the benefit of PET/MRI over PET/CT. Further studies are needed to determine the predictive value and potential indications of carotid PET/MRI in psoriasis patients.

Conclusion

Carotid PET/MRI is feasible in psoriatic patients for detection of atherosclerosis. The combination of PET and MRI enables acquisition of acute morphological and metabolic information without the need for ionizing radiation. Further studies in larger patient cohorts are required to evaluate the clinical utility of carotid PET/MRI in psoriatic patients.

Address correspondence to: Prabhakar Rajiah, Department of Radiology, University Hospital Cleveland Case Medical Center, Case Western Reserve University School of Medicine, Cleveland, Ohio, United States; Department of Radiology, Cardiothoracic Imaging, UT Southwestern Medical Center, Dallas, Texas, United States. E-mail: radprabhakar@gmail.com

References

- [1] Schon MP and Boehncke WH. Psoriasis. *N Engl J Med* 2005; 352: 1899-1912.
- [2] Gelfand JM, Weinstein R, Porter SB, Neimann AL, Berlin JA and Margolis DJ. Prevalence and Treatment of Psoriasis in the United Kingdom. *Arch Dermatol* 2005; 141: 1537-41.
- [3] Rachakonda TD, Schupp CW and Armstrong AW. Psoriasis prevalence among adults in the United States. *J Am Acad Dermatol* 2014; 70: 512-516.
- [4] Davidovici BB, Sattar N, Prinz J, Puig L, Emery P, Barker JN, van de Kerkhof P, Stahle M, Nestle FO, Girolomoni G and Krueger JG. Psoriasis and systemic inflammatory diseases: potential mechanistic links between skin disease and co-morbid conditions. *J Invest Dermatol* 2010; 130: 1785-1796.
- [5] Kagami S, Rizzo HL, Lee JJ, Koguchi Y and Blauvelt A. Circulating Th17, Th22, and Th1 cells are increased in psoriasis. *J Invest Dermatol* 2010; 130: 1373-1383.
- [6] Golden JB, Groft SG, Squeri MV, Debanne SM, Ward NL, McCormick TS and Cooper KD. Chronic Psoriatic Skin Inflammation Leads to Increased Monocyte Adhesion and Aggregation. *J Immunol* 2015; 195: 2006-2018.
- [7] Harden JL, Krueger JG and Bowcock AM. The immunogenetics of Psoriasis: A comprehensive review. *J Autoimmun* 2015; 64: 66-73.
- [8] Perera GK, Di Meglio P and Nestle FO. Psoriasis. *Annu Rev Pathol* 2012; 7: 385-422.
- [9] Parisi R, Rutter MK, Lunt M, Young HS, Symmons DP, Griffiths CE, Ashcroft DM; Identification and Management of Psoriasis Associated Comorbidity (IMPACT) project team. Psoriasis and the Risk of Major Cardiovascular Events: Cohort Study Using the Clinical Practice Research Datalink. *J Invest Dermatol* 2015; 135: 2189-2197.
- [10] Armstrong AW, Harskamp CT and Armstrong EJ. Psoriasis and the risk of diabetes mellitus: a systematic review and meta-analysis. *JAMA Dermatol* 2013; 149: 84-91.
- [11] Prodanovich S, Kirsner RS, Kravetz JD, Ma F, Martinez L and Federman DG. Association of psoriasis with coronary artery, cerebrovascular, and peripheral vascular diseases and mortality. *Arch Dermatol* 2009; 145: 700-703.
- [12] Gelfand JM, Dommasch ED, Shin DB, Azfar RS, Kurd SK, Wang X and Troxel AB. The risk of stroke in patients with psoriasis. *J Invest Dermatol* 2009; 129: 2411-2418.
- [13] Ahlehoff O, Gislason GH, Lindhardsen J, Olesen JB, Charlot M, Skov L, Torp-Pedersen C and Hansen PR. Prognosis following first-time myocardial infarction in patients with psoriasis: a Danish nationwide cohort study. *J Intern Med* 2011; 270: 237-244.
- [14] Gelfand JM, Neimann AL, Shin DB, Wang X, Margolis DJ and Troxel AB. Risk of myocardial infarction in patients with psoriasis. *JAMA* 2006; 296: 1735-1741.
- [15] Dasmahapatra P, Srinivasan SR, Mokha J, Fernandez C, Chen W, Xu J and Berenson GS. Subclinical Atherosclerotic Changes Related to Chronic Kidney Disease in Asymptomatic Black and White Young Adults: The Bogalusa Heart Study. *Ann Epidemiol* 2011; 21: 311-317.
- [16] Ripa RS, Knudsen A, Hag AM, Lebech AM, Loft A, Keller SH, Hansen AE, von Benzon E, Hojgaard L and Kjaer A. Feasibility of simultaneous PET/MR of the carotid artery: first clinical

Carotid PET/MRI in psoriasis patients

- experience and comparison to PET/CT. *Am J Nucl Med Mol Imaging* 2013; 3: 361-371.
- [17] Pedersen SF, Graebe M, Fisker Hag AM, Højgaard L, Sillesen H and Kjaer A. Gene expression and 18FDG uptake in atherosclerotic carotid plaques. *Nucl Med Commun* 2010; 31: 423-429.
- [18] Paspulati RM, Partovi S, Herrmann KA, Krishnamurthi S, Delaney CP and Nguyen NC. Comparison of hybrid FDG PET/MRI compared with PET/CT in colorectal cancer staging and restaging: a pilot study. *Abdom Imaging* 2015; 40: 1415-1425.
- [19] Silvera SS, Aidi HE, Rudd JH, Mani V, Yang L, Farkouh M, Fuster V and Fayad ZA. Multimodality imaging of atherosclerotic plaque activity and composition using FDG-PET/CT and MRI in carotid and femoral arteries. *Atherosclerosis* 2009; 207: 139-143.
- [20] Monteleone G, Pallone F, MacDonald TT, Chimenti S and Costanzo A. Psoriasis: from pathogenesis to novel therapeutic approaches. *Clin Sci (Lond)* 2011; 120: 1-11.
- [21] Chu B, Ferguson MS, Chen H, Hippe DS, Kerwin WS, Canton G, Yuan C and Hatsukami TS. Magnetic [corrected] resonance imaging [corrected] features of the disruption-prone and the disrupted carotid plaque. *JACC Cardiovasc Imaging* 2009; 2: 883-896.
- [22] Keller SH, Holm S, Hansen AE, Sattler B, Andersen F, Klausen TL, Højgaard L, Kjær A and Beyer T. Image artifacts from MR-based attenuation correction in clinical, whole-body PET/MRI. *MAGMA* 2012; 26: 173-181.
- [23] Samarin A, Burger C, Wollenweber SD, Crook DW, Burger IA, Schmid DT, von Schulthess GK and Kuhn FP. PET/MR imaging of bone lesions - implications for PET quantification from imperfect attenuation correction. *Eur J Nucl Med Mol Imaging* 2012; 39: 1154-1160.
- [24] Wiesmuller M, Quick HH, Navalpakkam B, Lell MM, Uder M, Ritt P, Schmidt D, Beck M, Kuwert T and von Gall CC. Comparison of lesion detection and quantitation of tracer uptake between PET from a simultaneously acquiring whole-body PET/MR hybrid scanner and PET from PET/CT. *Eur J Nucl Med Mol Imaging* 2013; 40: 12-21.
- [25] Keereman V, Holen RV, Mollet P and Vandenberghe S. The effect of errors in segmented attenuation maps on PET quantification. *Med Phys* 2011; 38: 6010-6019.
- [26] Bini J, Eldib M, Robson PM, Calcagno C and Fayad ZA. Simultaneous carotid PET/MR: feasibility and improvement of magnetic resonance-based attenuation correction. *Int J Cardiovasc Imaging* 2015; 32: 61-71.
- [27] Zaidi H, Ojha N, Morich M, Griesmer J, Hu Z, Maniowski P, Ratib O, Izquierdo-Garcia D, Fayad ZA and Shao L. Design and performance evaluation of a whole-body Ingenuity TF PET-MRI system. *Phys Med Biol* 2011; 56: 3091-3106.
- [28] Kalemis A, Delattre BM and Heinzer S. Sequential whole-body PET/MR scanner: concept, clinical use, and optimisation after two years in the clinic. The manufacturer's perspective. *MAGMA* 2013; 26: 5-23.
- [29] Bissonnette R, Tardif JC, Harel F, Pressacco J, Bolduc C and Guertin MC. Effects of the tumor necrosis factor-alpha antagonist adalimumab on arterial inflammation assessed by positron emission tomography in patients with psoriasis: results of a randomized controlled trial. *Circ Cardiovasc Imaging* 2013; 6: 83-90.
- [30] Evensen K, Slevolden E, Skagen K, Rønning OM, Brunborg C, Krogstad AL and Russell D. Increased subclinical atherosclerosis in patients with chronic plaque psoriasis. *Atherosclerosis* 2014; 237: 499-503.
- [31] Eder L, Jayakar J, Shanmugarajah S, Thavaneswaran A, Pereira D, Chandran V, Rosen CF and Gladman DD. The burden of carotid artery plaques is higher in patients with psoriatic arthritis compared with those with psoriasis alone. *Ann Rheum Dis* 2012; 72: 715-720.
- [32] Mehta NN. Systemic and Vascular Inflammation in Patients With Moderate to Severe Psoriasis as Measured by [18F]-Fluorodeoxyglucose Positron Emission Tomography-Computed Tomography (FDG-PET/CT). *Arch Dermatol* 2011; 147: 1031.
- [33] Rose S, Dave J, Millo C, Naik HB, Siegel EL and Mehta NN. Psoriatic arthritis and sacroiliitis are associated with increased vascular inflammation by 18-fluorodeoxyglucose positron emission tomography computed tomography: baseline report from the Psoriasis Atherosclerosis and Cardiometabolic Disease Initiative. *Arthritis Res Ther* 2014; 16: R161.
- [34] Bissonnette R, Tardif JC, Harel F, Pressacco J, Bolduc C and Guertin MC. Effects of the Tumor Necrosis Factor - Antagonist Adalimumab on Arterial Inflammation Assessed by Positron Emission Tomography in Patients With Psoriasis: Results of a Randomized Controlled Trial. *Circulation: Cardiovascular Imaging* 2012; 6: 83-90.
- [35] Dave J, Ahlman MA, Lockshin BN, Bluemke DA and Mehta NN. Vascular inflammation in psoriasis localizes to the arterial wall using a novel imaging technique. *J Am Acad Dermatol* 2014; 70: 1137-1138.
- [36] Bini J, Robson PM, Calcagno C, Eldib M and Fayad ZA. Quantitative carotid PET/MR imaging: clinical evaluation of MR-Attenuation correction versus CT-Attenuation correction in (18)F-FDG PET/MR emission data and com-

Carotid PET/MRI in psoriasis patients

- parison to PET/CT. *Am J Nucl Med Mol Imaging* 2015; 5: 293-304.
- [37] Wang J, Liu H, Sun J, Xue H, Xie L, Yu S, Liang C, Han X, Guan Z, Wei L, Yuan C, Zhao X and Chen H. Varying correlation between 18F-fluorodeoxyglucose positron emission tomography and dynamic contrast-enhanced MRI in carotid atherosclerosis: implications for plaque inflammation. *Stroke* 2014; 45: 1842-1845.
- [38] Saito H, Kuroda S, Hirata K, Magota K, Shiga T, Tamaki N, Yoshida D, Terae S, Nakayama N and Houkin K. Validity of Dual MRI and 18F-FDG PET Imaging in Predicting Vulnerable and Inflamed Carotid Plaque. *Cerebrovasc Dis* 2013; 35: 370-377.